Inorganic Chemistry

Article

pubs.acs.org/IC

Direct Observation of Bis(dicarbollyl)nickel Conformers in Solution by Fluorescence Spectroscopy: An Approach to Redox-Controlled Metallacarborane Molecular Motors

Alexander V. Safronov, Natalia I. Shlyakhtina, Thomas A. Everett, Monika R. VanGordon, Yulia V. Sevryugina, Satish S. Jalisatgi, and M. Frederick Hawthorne*

International Institute of Nano and Molecular Medicine, School of Medicine, University of Missouri, Columbia, Missouri 65211, United States

Supporting Information

ABSTRACT: As a continuation of work on metallacarborane-based molecular motors, the structures of substituted bis(dicarbollyl)nickel complexes in Ni^{III} and Ni^{IV} oxidation states were investigated in solution by fluorescence spectroscopy. Symmetrically positioned cage-linked pyrene molecules served as fluorescent probes to enable the observation of mixed meso-trans/*dl*-gauche (pyrene monomer fluorescence) and *dl*-cis/*dl*-gauche (intramolecular pyrene excimer fluorescence with residual monomer fluorescence) cage conformations of the nickelacarboranes in the Ni^{III} and Ni^{IV} oxidation states, respectively. The absence of energetically disfavored conformers in solution—*dl*-cis in the case of nickel(III) complexes and meso-trans in the case of nickel(IV)—was demonstrated based on spectroscopic data and conformer energy calculations in solution. The conformational persistence observed in solution indicates that bis(dicarbollyl)nickel complexes may provide attractive templates for building electrically driven and/or photodriven molecular motors.

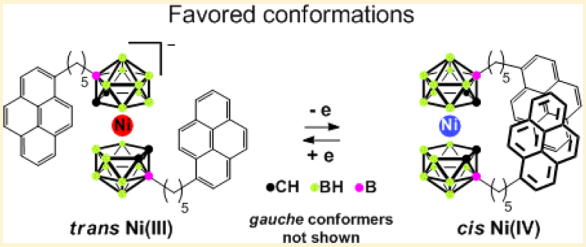

INTRODUCTION

Nanomachines represent a rapidly developing new area of the interdisciplinary field of nanoscience. Nanomachine research focuses on molecular-scale devices capable of converting either electrical or photo energy into mechanical motion that is translational, rotational, or both. While some artificial devices produce translational motion,[1] the most popular aspect of nanomachinery is likely the design and construction of molecular devices that exhibit controlled rotation of one part of the molecule with respect to another.[2] Depending on the degree and type of rotation control, these devices, also known as "molecular rotors" or "molecular motors" (the preferred term in this publication), can be classified as either Brownian (randomly rotating) or unidirectional. Molecular motor models have been constructed based on either purely organic templates,[3] including the use of DNA molecules,[4] or mixed organic/transition-metal moieties.[5] The use of transition-metal complexes or inorganic materials in the construction of molecular motors has been relatively limited.[6]

In 2004,[7] it was postulated that a well-known inorganic bis(dicarbollyl)nickel system (Figure 1) could be used as a template for building molecular motors with redox-controlled rotation. This nickelacarborane system exhibits the ability to change the formal oxidation state of the central nickel atom and in so doing controls the rotational confirmation of the complex.

Under ambient conditions, the central nickel atom can exist in two oxidation states, namely, Ni^{III} and Ni^{IV}. Transformations between the two oxidation states are reversible in solution through redox reactions accompanied by conformational changes of the carborane ligands from *meso-trans*-nickel(III) to *dl-cis*-nickel(IV), through the enantiomeric *dl*-gauche conformations. Calculated relative energies of conformations[7]

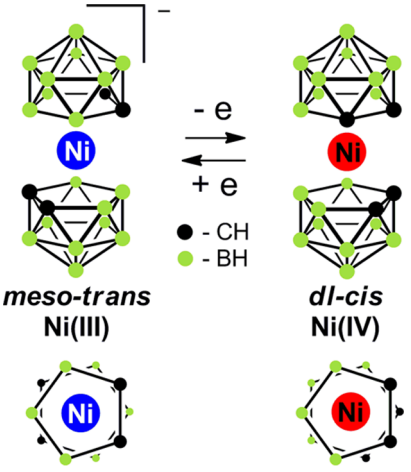

Figure 1. Schematic representation of the preferred conformational changes in nickelacarboranes associated with a change in the formal oxidation state of the central atom. For simplicity, *dl*-gauche conformers are not shown.

Received: September 19, 2013
Published: September 15, 2014

   dx.doi.org/10.1021/ic402372c | *Inorg. Chem.* 2014, 53, 10045−10053

for unsubstituted bis(dicarbollyl)nickel complexes of Ni^{III} and Ni^{IV} are presented in Table 1. It is important to note that the

Table 1. Calculated Relative Energies for *dl*-Cis, *dl*-Gauche, and Meso-Trans Conformers of Unsubstituted Bis(dicarbollyl)nickel Complexes of Ni^{III} and Ni^{IV} in Vacuum

	relative energy, kcal/mol	
conformer	Ni^{III}	Ni^{IV}
dl-cis	4.3	0
dl-gauche	1.0	0.9
meso-trans	0	3.0

charge, magnetic properties, electronic absorption spectrum, and polarity of the compounds also change with a change of the oxidation state of the central atom.

Density functional theory (DFT) studies[7] have also demonstrated that the energy of the highest occupied molecular orbital (HOMO) for the complex in the Ni^{IV} oxidation state is lowest in the *dl*-cis conformation and that this molecular orbital (MO) contains a bonding interaction between the two dicarbollide ligands. In contrast, the antibonding lowest unoccupied molecular orbital (LUMO) has a nodal plane through the central nickel atom. The reduction of Ni^{IV} to Ni^{III} places an electron in the LUMO, causing the dicarbollide ligands to adopt the meso-trans conformation to stabilize this orbital.

Conformational isomers of nickelacarboranes have been well-documented in the solid state by means of X-ray diffraction studies.[8] Although strong arguments exist in support of the conformational changes in solution, such as the high dipole moment of the nickel(IV) compound (6.5 D in benzene[9]), there have been no attempts to visualize such conformational changes by any type of solution spectroscopy. Confirmation of these conformational changes in solution is very important because molecular motors are intended to function in solution or at the interface of solid and liquid phases.[10]

Here, the use of a fluorescent molecular probe approach[11] to determine nickelacarborane conformations in solution is presented. Fluorescent molecular probes are widely used in biochemistry to determine the proximity of different parts of protein and DNA molecules.[12] Among a number of fluorescent probes available, pyrene—a polycyclic condensed aromatic system containing four fused benzene rings—was very attractive for our studies. Once excited by UV light, pyrene is able to form a short-lived excited-state dimer, also known as an *excimer*, with a neighboring pyrene molecule. The excimer fluoresces at a longer wavelength than the pyrene monomer, and its broad and shapeless band profile makes it easily distinguishable. Usually, pyrene excimers form only if the two participating pyrene molecules are located within a certain distance (usually 3.5−4.5 Å) and are properly oriented with respect to each other.

If the two equivalent pyrene molecules in a nickelacarborane system are symmetrically attached to both carborane cages by saturated flexible linkers (Figure 2), they will be able to form explicit *intramolecular* excimers only in the case of the enantiomeric *dl*-cis conformations in the nickel(IV) complex (Figure 2, bottom row) because of the proximity of one pyrene with another. For the nickel(III) complex, only the fluorescence of the pyrene monomer will be observed because the pyrenes will be too separated from each other to form an excimer when present in either the meso-trans or *dl*-gauche conformation (Figure 2, top row). The possibility of *intermolecular* excimer formation was also considered because, unlike solutions of proteins, organic polymers, or DNA, in which the formation of intermolecular excimers is extremely unlikely and can be neglected, metallacarborane molecules are small enough to participate in these bimolecular interactions.

RESULTS

To directly observe nickelacarborane conformations in solution, a series of substituted nickelacarboranes were prepared in which pyrene molecules were attached to the boron atoms of carborane cages by means of alkylene linkers. Preparing carboranes with such linkers is relatively easy, and the linker

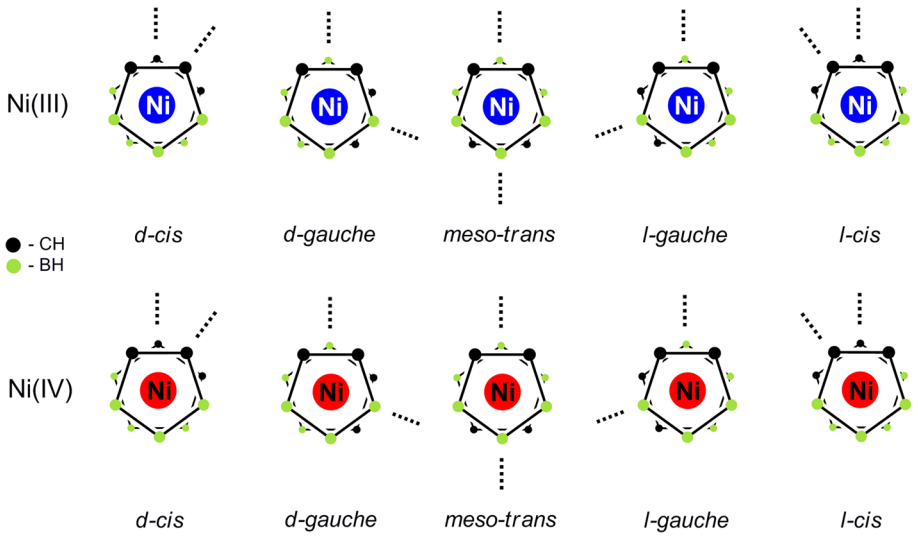

Figure 2. Schematic representations of possible conformations adopted by symmetrically 3,3′-disubstituted nickel(III) and -(IV) complexes in solutions. Dashed lines mark the positions of the pyrenylalkyl substituents. The assignment of structures as *d* and *l* was based on an arbitrary arrangement.

dx.doi.org/10.1021/ic402372c | *Inorg. Chem.* 2014, 53, 10045−10053

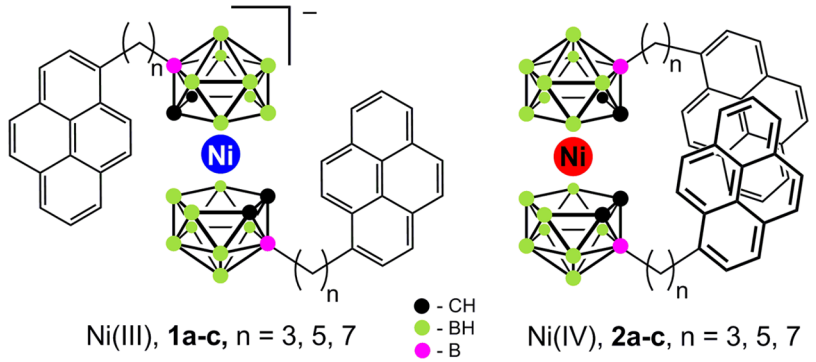

Figure 3. Pyrene-substituted nickelacarborane complexes **1a**−**1c** and **2a**−**2c**.

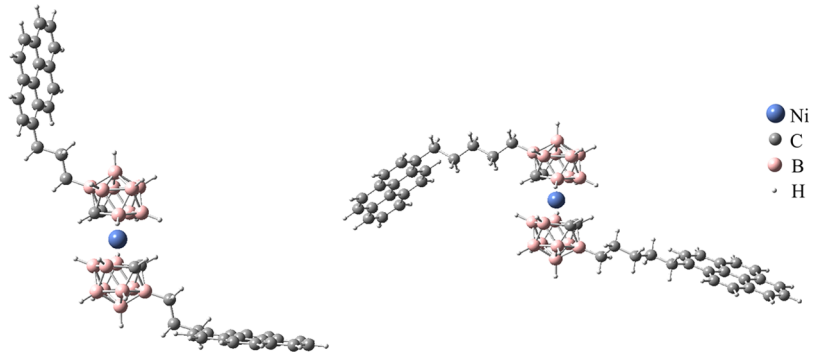

Figure 4. Optimized structures of the nickel(III) complexes **1a** (left) and **1b** (right) in acetonitrile.

length can be varied while maintaining the same synthetic methodology. In addition, saturated alkyl chains are not fluorescent, and they prevent electron transfer through the carborane cage, thus avoiding possible distortions in the fluorescence spectra. The flexibility of the alkylene linkers also allows the pyrene molecules to adopt the spatial orientation necessary for efficient excimer formation.

A potential problem with the proposed experimental design is the fluorescence quenching ability of nickel compounds.[13] Although most quenching studies have dealt with inorganic and organometallic derivatives of nickel(II), it was important to eliminate the possibility of quenching for the nickel(III) and -(IV) metallacarborane complexes presented here. Before the syntheses of pyrene-substituted nickelacarboranes are undertaken, the pyrene fluorescence in the presence of both unsubstituted nickel(III) and -(IV) metallacarborane complexes was examined. To clearly observe both the pyrene monomer and excimer, the fluorescence spectra of a 10^{-3} M pyrene solution containing unsubstituted nickelacarboranes in the Ni^{III} and Ni^{IV} oxidation states at a concentration of 5×10^{-4} M were measured. In both cases, the emission intensities of the pyrene monomer and excimer had decreased compared to the spectra of pure pyrene at the same concentration, but the shapes and intensity ratios of the bands were distinct and remained virtually unchanged. These results were encouraging for continuation of the study of the target nickelacarboranes.

Molecular modeling studies were employed to predict the number of methylene groups needed to connect the nickelacarborane core and the pyrene substituent that would provide an optimal spatial distribution of the pyrene molecules for effective intramolecular excimer formation.

1. Molecular Modeling. Three pairs of compounds, shown schematically in Figure 3, with tri-, penta-, and heptamethylene linkers separating the carborane cages and the pyrene molecules were modeled. Linker lengths were chosen based on the synthetic availability of the corresponding pyrene compounds.

DFT calculations for compounds **1a**−**1c** and **2a**−**2c** at the B3LYP/6-31G(d) level of theory were performed in acetonitrile (conductor-like polarizable continuum model)[14] using the *Gaussian09* suite of programs.[15] An acetonitrile solvent was chosen for the reasons described in parts 5 and 6 of this paper. Several initial configurations that differed in the dihedral angle distribution in the alkylene chains were subjected to energy minimization. The optimized structures of the nickel(III) (**1a** and **1b**) and nickel(IV) (**2a** and **2b**) compounds were in the minima of the potential energy hypersurface, as confirmed by the lack of imaginary frequencies in the energy second derivative matrixes. Stabilization of the molecules containing seven methylene groups (**1c** and **2c**) in the chosen basis set was unsuccessful. The most negative total energy conformations of compounds **1a**, **1b**, **2a**, and **2b** were chosen for further analysis and are described below.

The calculated structures of the formal nickel(III) complexes **1a** and **1b** are shown in Figure 4. In both complexes, the energy minimum corresponds to the meso-trans conformation, in which the pyrenylalkyl substituents are extended toward opposite sides of the metallacarborane moiety. Any intramolecular interaction between the pyrene substituents can most likely be ruled out.

In the optimized structures of the formal nickel(IV) complexes **2a** and **2b**, the cages adopt *dl*-cis conformations, bringing the pyrenylalkyl substituents together. The distances between the mass centers of the two pyrene fragments are 7.6 Å in **2a** and 7.9 Å in **2b** (Figure 5). In structure **2a**, the pyrene substituents are almost perpendicular to each other, forming a T-shaped configuration. In compound **2b**, the substituents form

dx.doi.org/10.1021/ic402372c | *Inorg. Chem.* 2014, 53, 10045−10053

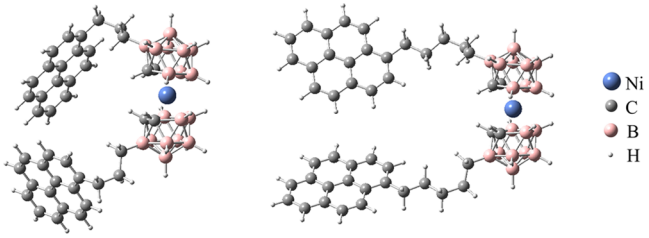

Figure 5. Optimized structures of the nickel(IV) complexes **2a** (left) and **2b** (right) in acetonitrile.

a slipped-parallel or, in other terms, a parallel-displaced configuration.

Despite the proximity of the substituents in compound **2a**, the alkylene chain flexibility is limited, which could result in an unfavorable spatial arrangement of the pyrenes for effective excimer formation. Complex **2b** would be the most favorable candidate for observing an *intramolecular* excimer if solvation enabled substituent proximity. The possibility of intramolecular excimer formation in the case of compound **2c** was questionable because of the excessive flexibility of the linker.

2. Synthesis of Metallacarborane Compounds. The computational simulation results were quite informative; on the basis of these results, syntheses of the target nickelacarboranes **1** and **2**, starting from the preparation of the substituted pyrenes bearing terminal alkenyl chains, were initiated.

2.1. Synthesis of Substituted Pyrenes. The compound 1-allylpyrene (**4**) was prepared in 80% isolated yield by a cross-coupling reaction between 1-bromopyrene (**3**) and allylmagnesium bromide in tetrahydrofuran (THF) in the presence of a palladium(0) catalyst (Scheme 1).

Scheme 1. Synthesis of 4

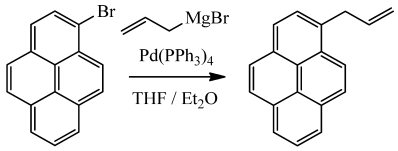

The synthesis of 1-(pent-4-en-1-yl)pyrene (**7**) was achieved in two steps starting from commercially available 1-pyrenylbutanol (**5**), which was first oxidized to 4-(pyren-1-yl)butanal (**6**) by pyridinium chlorochromate (PCC) in dichloromethane (DCM). The resulting aldehyde **6** was then introduced into a Wittig reaction with in situ generated methylenetriphenylphosphorane to give **7** with an overall yield of 60% (Scheme 2).

The synthesis of the longest chain congener, 1-(hept-6-en-1-yl)pyrene (**9**), was performed starting from **5** with the initial formation of the bromide **8**. Subsequent reaction of the intermediate alkylcuprate derivative of **8** with allylmagnesium bromide in THF generated **9** in 48% yield, as shown in Scheme 3. The purity and identity of the target and intermediate

Scheme 2. Synthesis of 7

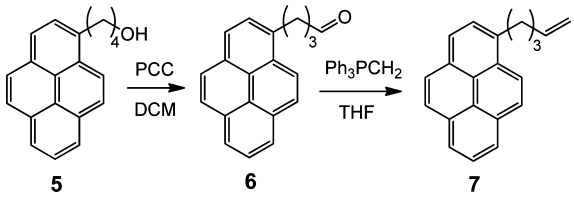

Scheme 3. Synthesis of 9

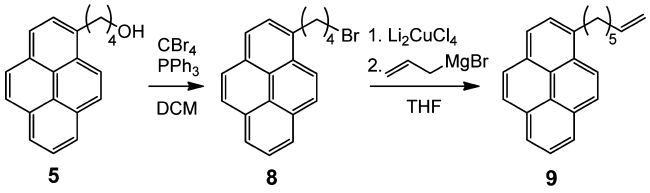

compounds **4** and **6**–**9** were established based on multinuclear NMR and high-resolution mass spectrometry (HRMS) data (see the Supporting Information, SI).

2.2. Synthesis of Substituted closo- and nido-Carboranes. The corresponding substituted *closo*-carboranes **10a**–**10c** were synthesized according to the recently discovered strategy,[16] which includes the in situ preparation of alkyldichloroboranes via hydroboration of the terminal alkenes with the $HBCl_2$·L complex and subsequent insertion of the alkyldichloroborane into thallium dicarbollide.

Initially, a hydroboration reaction of alkenes **4**, **7**, and **9** with the $HBCl_2$·dioxane complex was attempted, but the reaction proceeded very slowly, even at elevated temperatures. After several hydroborating agents and techniques were screened, it was determined that the best results were achieved by BCl_3-assisted hydroboration[17] of **4**, **7**, and **9** by the $HBBr_2$·SMe_2 complex in DCM (Scheme 4). The reaction of the resulting alkyldibromoboranes with thallium dicarbollide generated the target *closo*-carboranes **10a**–**10c** in good yield. Closo compounds **10a**–**10c** were deboronated by tetrabutylammonium fluoride to generate the corresponding *nido*-carboranes **11a**–**11c** in quantitative yield. All compounds were characterized by NMR and HRMS (see the SI).

2.3. Synthesis of Nickelacarboranes. Nickelacarborane compounds of formal nickel(III) **1a**–**1c** were prepared in good yield by the reaction of *nido*-carboranes **11a**–**11c**, which were initially deprotonated by *t*BuOK, with nickel acetylacetonate [$Ni(acac)_2$] in anhydrous THF (Scheme 5). The products were isolated from the reaction mixtures by column chromatography.

Oxidation of complexes **1a**–**1c** by 1 equiv of aqueous $FeCl_3$ in acetonitrile generated the corresponding complexes **2a**–**2c** in good-to-excellent yields. Multinuclear NMR data were collected for all nickel(IV) complexes, which, along with the HRMS results, confirmed their purity and identity (see the SI).

3. Electrochemical Studies. Nickelacarboranes can exist in three possible formal oxidation states of the nickel atom: II+, III+, and IV+. However, dianionic diamagnetic bis(dicarbollyl) complexes of nickel(II) are quickly oxidized in air both in the solid state and in solution to produce more stable paramagnetic complexes of nickel(III). The latter is also oxidized much more slowly in air both in the solid state and in solution to form stable diamagnetic nickel(IV) species. A typical cyclic voltammogram (CVA) for a nickelacarborane contains two peaks corresponding to the reversible transformations $Ni^{II} \leftrightarrow Ni^{III}$ and $Ni^{III} \leftrightarrow Ni^{IV}$.

Cyclic voltammetry of solutions of the nickel(III) complexes **1a**–**1c** in degassed acetonitrile revealed reversible oxidation–reduction peaks corresponding to $Ni^{III} \leftrightarrow Ni^{IV}$ transformations (see the SI). Half-wave potentials for compounds **1a**–**1c** versus

dx.doi.org/10.1021/ic402372c | Inorg. Chem. 2014, 53, 10045–10053

Scheme 4. Synthesis of *closo*- and *nido*-Carborane Intermediates

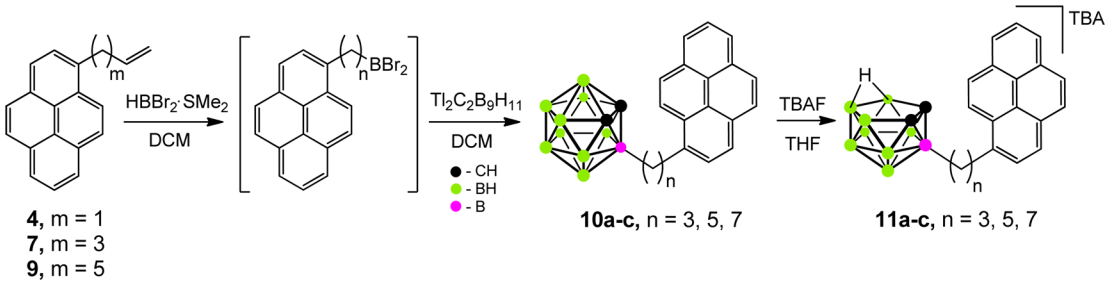

Scheme 5. Synthesis of Pyrene-Substituted Nickelacarborane Complexes

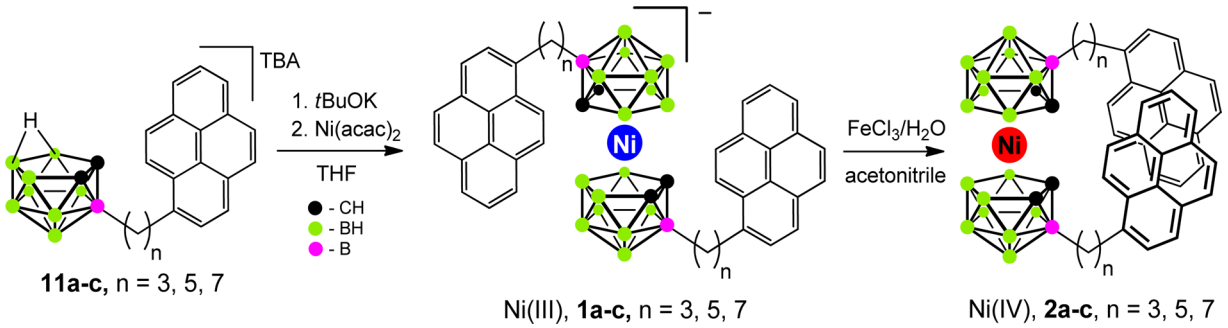

the Fc^+/Fc couple were −225, −231, and −232 mV, respectively. These values are comparable with the $Ni^{III} \leftrightarrow Ni^{IV}$ redox potential of −217 mV determined for unsubstituted bis(dicarbollyl)nickel.[9] The undistorted CVA demonstrated that (1) the electrochemical behavior of the substituted nickelacarborane core in compounds **1** and **2** is predictable and normal and (2) the pyrenes and linkers do not participate in the electrochemical reactions of the nickelacarborane core.

4. UV−Vis and Spectroelectrochemical Studies. In the UV region, a characteristic absorption peak for the unsubstituted nickel(III) nickelacarborane core has been identified at 320−340 nm, while nickel(IV) absorbs at 290−300 nm.[9] Pyrene usually displays three major absorption bands with maxima at 240, 275, and 350 nm.[18]

The UV−vis spectra of the nickel(III) complexes **1a−1c** measured in degassed acetonitrile exhibited only three groups of absorption peaks, characteristic of pyrene. Because the strongest absorption of the nickelacarborane core in the formal Ni^{III} oxidation state lies within the 320−340 nm range, it overlaps with that of the pyrene absorptions centered at 350 nm. In the UV spectra of the nickel(IV) complexes **2a−2c**, a weak absorption band at 300 nm, characteristic of the nickel(IV) core, was observed along with the characteristic pyrene peaks (see the SI).

Spectroelectrochemical experiments in acetonitrile showed characteristic changes in the UV spectra upon oxidation of the formal nickel(III) compounds **1a−1c** to the nickel(IV) complexes **2a−2c**. For example, during the controlled electrochemical oxidation of compound **1b** in a UV cell, a band appeared at 300 nm, corresponding to the absorption of the formal nickel(IV) core. Electrochemical reduction of the resulting compound **2b** restored the absorption spectrum to its original state. This experiment confirmed that the presence of the nickelacarborane core does not interfere with the spectral properties of pyrene (see the SI).

5. Fluorescence Spectroscopy Study of the Nickel(III) Complexes 1a−1c. Fluorescence spectroscopic measurements of nickel(III) complexes **1a−1c** were conducted with an excitation wavelength of 360 nm. This wavelength, although not the wavelength corresponding to the peak of the pyrene absorption band, is reported to correspond to the direct $S_0 \rightarrow S_1$ transition of the pyrene molecule.[18] In addition, the choice of the 360 nm wavelength helped to minimize absorption by the nickel(III) core.

The choice of solvent was also very important in this study. The fluorescence of both the pyrene monomer and excimer is very sensitive to solvent polarity, viscosity, and the presence of radical quenchers. The solubility of complexes **1a−1c** and **2a−2c** also limits the choice of solvents. Fluorescence spectra of complexes **1a−1c** and **2a−2c** in degassed anhydrous acetonitrile, THF, and toluene at temperatures ranging from −10 to +50 °C showed negligible temperature dependence. As such, this issue will not be discussed further.

Emission spectra of nickel(III) complexes **1a−1c** at a concentration of 10^{-3} M revealed only a low-intensity broad band centered at 500 nm. The spectra were measured in a 1 mm cuvette to avoid the inner filter effect, revealing a combination of pyrene monomer fluorescence and a broad band centered at 500 nm. Interestingly, 10-fold dilution resulted in an immediate dramatic effect on the emission. Spectra of **1b** measured at a concentration of 10^{-4} M showed only well-resolved fluorescence of the pyrene monomer and the complete disappearance of the initial broad signal at 500 nm (Figure 6). Spectra obtained at even lower concentrations, as low as 10^{-7} M, showed no further variation. The disappearance of the 500 nm emission band of the diluted solutions allowed the assignment of this band to *intermolecular* excimer formation at a concentration of 10^{-3} M.

6. Fluorescence Spectroscopy Study of Nickel(IV) Complexes 2a−2c. Fluorescence spectra of nickel(IV) complexes **2a−2c** measured at concentrations of 10^{-3} M in degassed acetonitrile, THF, and toluene showed trends similar to those of the corresponding nickel(III) complexes. The spectra revealed only a broad low-intensity emission band

dx.doi.org/10.1021/ic402372c | *Inorg. Chem.* 2014, 53, 10045−10053

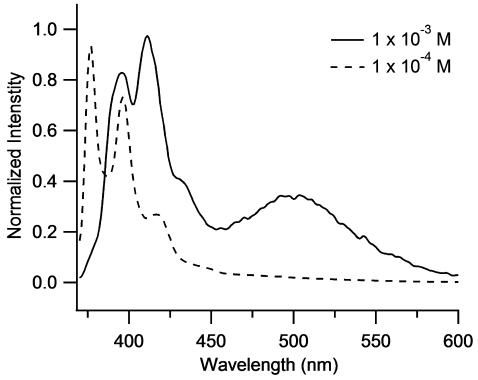

Figure 6. Normalized fluorescence spectra of complex **1b** measured at concentrations of 10^{-3} M (solid line, 1 mm cuvette, acetonitrile, 293 K, and λ_{ex} = 360 nm) and 10^{-4} M (dashed line, 10 mm cuvette, acetonitrile, 293 K, and λ_{ex} = 360 nm).

centered at 500 nm, corresponding to intermolecular excimer formation.

As observed for the nickel(III) complexes diluted to a concentration of 10^{-4} M, the broad band at 500 nm also disappeared in the spectra of nickel(IV) complexes **2a**–**2c**. At this concentration, the spectra of all three nickel(IV) complexes in toluene and the spectra of complexes **2a** and **2c** in acetonitrile and THF contained only signals attributed to fluorescence of the pyrene monomer. However, in the fluorescence spectra of **2b** measured at a concentration of 10^{-4} M in acetonitrile and THF, a new unresolved band centered at 450 nm (more pronounced in acetonitrile and less visible in THF) was observed, along with fluorescence of the pyrene monomer (Figure 7). The broadness and absence of fine structure in this new band suggest that it belongs to a different type of excimer.

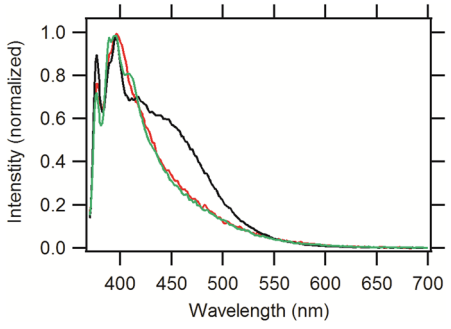

Figure 7. Normalized fluorescence spectra of complexes **2a** (green), **2b** (black), and **2c** (red) at a concentration of 10^{-4} M (acetonitrile, 293 K, and λ_{ex} = 360 nm).

The new excimer band at 450 nm was blue-shifted by approximately 50 nm compared to the intermolecular 500 nm excimer band. Such a spectral shift in the case of pyrene excimers has previously been observed for pyrenes attached to a common core[19] and has been assigned to the excimer formed by partially overlapping pyrene molecules in a parallel-displaced configuration. The band at 500 nm is usually attributed to the symmetrical sandwich-like dimer, which can be formed in an intermolecular fashion by pyrenes attached to different molecules. Because of the constrained nature of the substituents in compound **2b** revealed by the DFT calculations, the parallel-displaced configuration of the pyrenes is preferable in this case, and, consequently, observation of the blue-shifted excimer band upon dilution indicates formation of the *intramolecular* excimer.

As mentioned previously, it was anticipated that both the length of the linker connecting the pyrene fragment to the nickelacarborane cage and the choice of the solvent for the fluorescence study would play a crucial role in the successful observation of nickelacarborane conformations in solution. The initial fluorescence measurements demonstrated that the length of the pentamethylene linker is optimal for *intramolecular* pyrene excimer formation. Observation of the most intense intramolecular excimer band in acetonitrile is also quite reasonable. The excimer formation process has long been defined as a "diffusion-controlled collision" process.[20] Of acetonitrile, THF, and toluene, acetonitrile is the least viscous solvent, while toluene is the most viscous. Thus, the data suggest that it might be the ease of diffusion that made the initial observation of intramolecular excimer formation successful in acetonitrile and unsuccessful in toluene. Another possible reason is the affinity of pyrene to toluene precluding the excimer formation. It is important to reemphasize that the choice of solvents was also limited by the actual solubility of the nickelacarboranes that were investigated.

After it was determined that complex **2b** was the optimal compound and acetonitrile was the optimal solvent, the study was continued by measuring the concentration dependence of the fluorescence spectra of complex **2b** (Figure 8). The largest

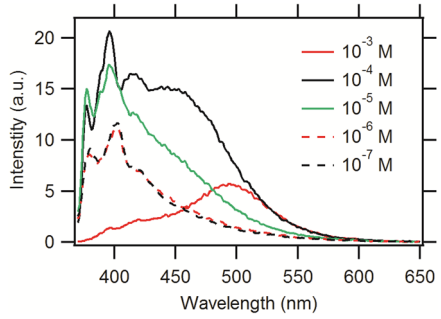

Figure 8. Concentration dependence of the fluorescence spectra of compound **2b** (acetonitrile, 293 K, and λ_{ex} = 360 nm).

change in the spectra occurred upon dilution from 10^{-3} to 10^{-4} M, when a new band centered at 450 nm appeared while the emission band of the *intermolecular* excimer became undetectable. The clearest observations of the *intramolecular* excimer band for compound **2b** were recorded at concentrations of 10^{-4}–10^{-5} M. At 10^{-6} M, the intensity of the excimer band decreased significantly, and further dilution to a concentration of 10^{-7} M revealed no change in the band intensity.

To further confirm the assumptions that the 450 nm band is attributable to the formation of the intramolecular excimer and the 500 nm band is attributable to the formation of the intermolecular excimer, the bis(dicarbollyl)nickel(IV) complex **14** was prepared (Scheme 6); the compound contains a single pyrene substituent connected to the dicarbollide cage with a pentamethylene linker. Because this complex lacks the second pyrene substituent, it is only capable of intermolecular excimer formation. The synthesis of compound **13** starting from *nido*-carboranes **11b** and **12** is depicted in Scheme 6 (see the SI). Compound **13** was isolated by chromatographic techniques from the two symmetrical byproducts, namely, complex **1b** and

dx.doi.org/10.1021/ic402372c | Inorg. Chem. 2014, 53, 10045–10053

Scheme 6. Synthesis of the Monosubstituted Nickelacarboranes 13 and 14

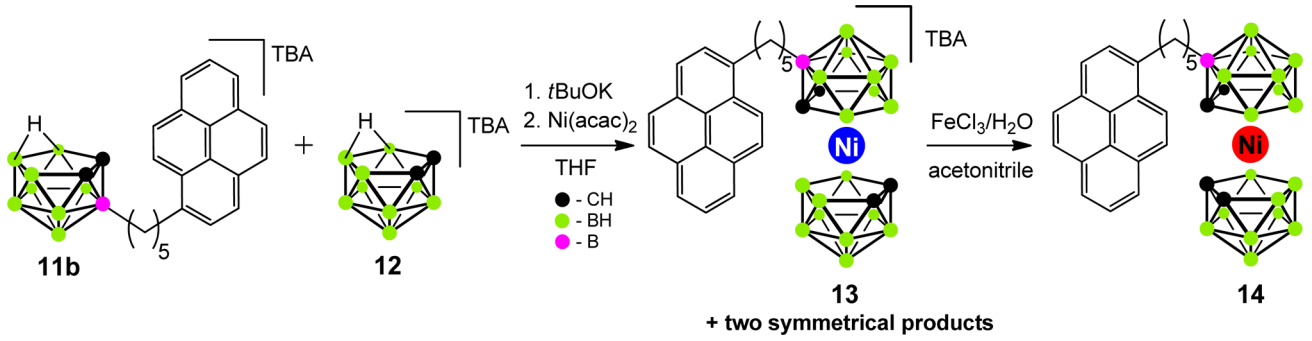

the parent bis(dicarbollyl)nickel. Oxidation of **13** in acetonitrile with aqueous $FeCl_3$ generated compound **14** in quantitative yield.

Fluorescence spectra of compound **14** measured in acetonitrile at a concentration of 10^{-3} M showed a broad, featureless band centered at 500 nm, consistent with the formation of the intermolecular excimer. Upon dilution to concentrations in the range of 10^{-4}–10^{-6} M in acetonitrile, the spectra of compound **14** showed only pyrene monomer fluorescence. A comparison of the fluorescence spectra of compounds **2b** and **14** in acetonitrile at a concentration of 10^{-4} M is shown in Figure 9.

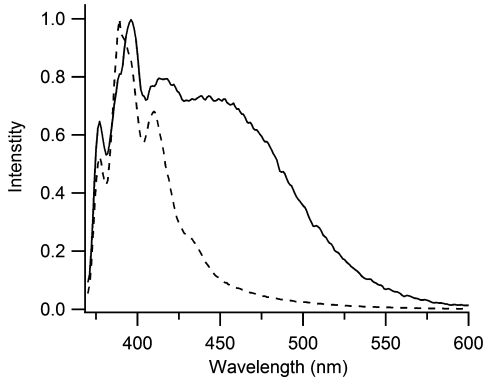

Figure 9. Normalized fluorescence spectra of compounds **2b** (solid) and **14** (dashed) at a concentration of 10^{-4} M (acetonitrile, 293 K, and λ_{ex} = 360 nm).

DISCUSSION

The general purpose of this study was to determine the applicability of the nickelacarborane unit as a template for the construction of molecular switch/motor-type devices. For this purpose, the conformational assignment of the fluorescent molecular-probe-labeled nickel(III) and -(IV) nickelacarboranes in solutions was attempted. It was demonstrated that at concentrations higher than 10^{-4} M both nickel(III) and -(IV) compounds exhibit fluorescence characteristic for the formation of intermolecular excimers that was additionally complicated by the inner filter effect. Further discussion will be limited to (1) the nickel(III) complex **1b** and the nickel(IV) complex **2b** because only these complexes revealed sufficient spectral information to permit conformational analysis and (2) the concentration range 10^{-4}–10^{-7} M.

It was demonstrated[7] that in vacuum the plot of the potential energy dependence on the rotational angle contains three energy minima for both unsubstituted nickel(III) and -(IV) metallacarboranes. These minima correspond to specific conformations—meso-trans, *dl*-gauche, or *dl*-cis—adopted by cage carbon atoms with respect to each other (Figure 2). For the nickel(III) compound, relative energies of conformers increase in the order meso-trans → *dl*-gauche → *dl*-cis, while for the nickel(IV) compound, relative energies increase in the order *dl*-cis → *dl*-gauche → meso-trans (Table 1).

A similar dependence of the potential energy on the rotational angle is observed for the substituted compounds **1b** and **2b** in solution. In Table 2, calculated relative energies of

Table 2. Calculated Relative Energies for *dl*-Cis, *dl*-Gauche, and Meso-Trans Conformers of Bis(dicarbollyl)nickel Complexes 1b (Ni^{III}) and 2b (Ni^{IV}) at 293 K in Acetonitrile

	relative energy, kcal/mol	
conformer	**1b** (Ni^{III})	**2b** (Ni^{IV})
dl-cis	10.6	0
dl-gauche	0.1	1.2
meso-trans	0	14.0

dl-cis, *dl*-gauche, and meso-trans conformers of nickelacarboranes **1b** and **2b** in acetonitrile at 293 K are shown (see the SI for details of the computational studies). The calculated energy differences between the most stable conformers—meso-trans for nickel(III) and *dl*-cis for nickel(IV)—and the neighboring *dl*-gauche conformers are relatively low: 0.1 kcal/mol for the meso-trans → *dl*-gauche transition in the nickel(III) complex **1b** and 1.2 kcal/mol for the *dl*-cis → *dl*-gauche transition in the nickel(IV) complex **2b**. For transitions meso-trans → *dl*-cis for **1b** and *dl*-cis → meso-trans for **2b**, energy differences are significantly higher −10.6 and 14.0 kcal/mol, respectively.

Using the Boltzmann equation (see the SI), it was possible to calculate ratios of *dl*-cis, *dl*-gauche, and meso-trans conformers of compounds **1b** and **2b** in acetonitrile at 293 K (the temperature of fluorescence studies). As can be seen from Table 3, statistical mechanics data suggest that nickel(III) complex **1b** exists in an acetonitrile solution at 293 K as a 54:46 mixture of meso-trans and *dl*-gauche conformers; the amount

Table 3. Calculated Ratios for *dl*-Cis, *dl*-Gauche, and Meso-Trans Conformers of Bis(dicarbollyl)nickel Complexes 1b (Ni^{III}) and 2b (Ni^{IV}) in Acetonitrile at 293 K

	dl-cis, %	*dl*-gauche, %	meso-trans, %
1b	9.5×10^{-7}	46.4	53.6
2b	88.1	11.9	4.5×10^{-9}

dx.doi.org/10.1021/ic402372c | *Inorg. Chem.* 2014, 53, 10045−10053

of the *dl*-cis conformers of **1b** at 293 K in acetonitrile is very low. At the same time, nickel(IV) complex **2b** exists in acetonitrile at 293 K as a mixture of *dl*-cis and *dl*-gauche conformers in an approximate 88:12 ratio. The amount of the meso-trans conformer in an acetonitrile solution of **2b** at 293 K is negligible.

The results of calculations are supported by the spectroscopic observations. For example, fluorescence spectra of nickel(III) complex **1b** at 293 K in acetonitrile showed only pyrene monomer fluorescence signals with no excimer peaks detected. Because of the increased distance between the pyrene substituents, both meso-trans and *dl*-gauche conformers of **1b** would produce only monomer emission; distinguishing between these conformers by spectroscopic methods would be impossible. Therefore, it is reasonable to suggest that compound **1b** exists in solutions as a mixture of meso-trans and *dl*-gauche conformers. The extremely low calculated content of the *dl*-cis conformer of **1b** in acetonitrile at 293 K (9.5×10^{-7}%; Table 3) explains the absence of an intramolecular excimer band in spectra of **1b** and suggests that the concentration of *dl*-cis conformers of **1b** in the solution is very low, below the detection threshold of the spectrometer.

Fluorescence spectra of the nickel(IV) complex **2b** in acetonitrile in the concentration range of 10^{-4}–10^{-7} M (Figure 8) revealed—along with the residual emission of the pyrene monomer—a broad unresolved band centered at 450 nm that was attributed to the intramolecular pyrene excimer. This observation is in agreement with the calculated Boltzmann distribution of conformers of **2b** in acetonitrile at 293 K, giving a ratio of *dl*-cis and *dl*-gauche conformers of approximately 88:12 (Table 3). It may be concluded that compound **2b** exists in an acetonitrile solution at 293 K as a mixture of *dl*-cis and *dl*-gauche conformers. However, it is important to emphasize that the presence of *dl*-gauche conformers is not the only factor that may contribute to the appearance of the pyrene monomer fluorescence in the emission spectra of **2b**. The excimer formation is strongly dependent on the respective orientation of the pyrene substituents. Therefore, at any given moment, the spatial orientation necessary for efficient excimer formation will be adopted by the pyrene substituents only in a subset of molecules of **2b** in the *dl*-cis conformation. Without being properly oriented, these pyrene substituents contribute to monomer fluorescence. Although it is impossible to estimate the contribution of meso-trans conformers to the fluorescence spectra of **2b** based solely on spectroscopy data, calculations predict that their content in acetonitrile solutions of **2b** at 293 K is extremely low (4.5×10^{-9}%; Table 3).

CONCLUSIONS

In summary, the conformations of bis(dicarbollyl)nickel complexes in the Ni^{III} and Ni^{IV} oxidation states were studied in solution using fluorescence spectroscopy. A number of nickel(III) and -(IV) complexes bearing fluorescent pyrenylalkyl substituents were synthesized, and their ability to form pyrene excimers was examined. As expected, an intramolecular pyrene excimer emission was observed for the nickel(IV) complex, while the corresponding nickel(III) complex revealed only monomer fluorescence. On the basis of the spectroscopic data, the calculated energies of conformers, and their concentrations calculated using the Boltzmann distribution, it can be concluded that the bis(dicarbollyl)nickel complex in the formal Ni^{III} oxidation state exists in solution as a mixture of meso-trans and *dl*-gauche conformers, while the corresponding nickel(IV) complex exists as a mixture of *dl*-cis and *dl*-gauche conformers. These studies indicate that nickelacarboranes may provide attractive templates for electro- or photocontrolled molecular motor/switch-type devices.

ASSOCIATED CONTENT

Supporting Information

X-ray crystallographic data in CIF format, experimental procedures, NMR data, and spectra for all prepared compounds, X-ray data for **2b**, CVA and spectroelectrochemistry data, UV and fluorescence spectra of compounds **1** and **2**, as well as the details of DFT simulations. This material is available free of charge via the Internet at http://pubs.acs.org.

AUTHOR INFORMATION

Corresponding Author

*E-mail: hawthornem@missouri.edu. Phone: 573-882-7016. Fax: 573-884-6900.

Notes

The authors declare no competing financial interest.

ACKNOWLEDGMENTS

We thank Dr. Timothy Glass (Department of Chemistry, University of Missouri—Columbia) for helpful discussions, Brett Meyers and James Woody for measuring the mass spectra of prepared compounds, and Pamela Cooper for manuscript editing.

REFERENCES

(1) See for example: (a) Karpal, R. *J. Chem. Phys.* **2013**, *138*, 020901. (b) Brouwer, A. M.; Frochot, C.; Gatti, F. G.; Leigh, D. A.; Mottier, L.; Paolucci, F.; Roffia, S.; Wurpel, G. W. H. *Science* **2001**, *291*, 2124.

(2) (a) Browne, W. R.; Feringa, B. L. *Nat. Nanotechnol.* **2006**, *1*, 25. (b) Davis, A. P. *Nature* **1999**, *401*, 120.

(3) (a) Fletcher, S. P.; Dumur, F.; Pollard, M. M.; Feringa, B. L. *Science* **2005**, *310*, 80. (b) Harada, A. *Acc. Chem. Res.* **2001**, *34*, 456.

(4) Mao, C.; Sun, W.; Shen, Z.; Seeman, N. C. *Nature* **1999**, *397*, 144.

(5) (a) Amendola, V.; Fabrizzi, L.; Mangano, C.; Pallavicini, P. *Acc. Chem. Res.* **2001**, *34*, 488. (b) Collin, J.-P.; Dietrich-Buchecker, C.; Gaviña, P.; Jimenez-Molero, M. C.; Sauvage, J.-P. *Acc. Chem. Res.* **2001**, *34*, 477.

(6) Kottas, G. S.; Clarke, L. I.; Horinek, D.; Michl, J. *Chem. Rev.* **2005**, *105*, 1281.

(7) Hawthorne, M. F.; Zink, J. I.; Skelton, J. M.; Bayer, M. J.; Liu, C.; Livshits, E.; Baer, R.; Neuhauser, D. *Science* **2004**, *303*, 1849 . See also calculations presented in the SI.

(8) (a) St. Clair, D.; Zalkin, A.; Templeton, D. H. *J. Am. Chem. Soc.* **1970**, *92*, 1173. (b) Hawthorne, M. F.; Dunks, G. B. *Science* **1972**, *178*, 462.

(9) Warren, L. F., Jr.; Hawthorne, M. F. *J. Am. Chem. Soc.* **1970**, *92*, 1157.

(10) Vogelsberg, C. S.; Garcia-Garibay, M. A. *Chem. Soc. Rev.* **2012**, *41*, 1892 and references therein.

(11) Kolpashchikov, D. M. *Chem. Rev.* **2010**, *110*, 4709.

(12) See for example: Li, Y.; Zhou, X.; Ye, D. *Biochem. Biophys. Res. Commun.* **2008**, *373*, 457.

(13) See for example: (a) Varnes, A. V.; Dodson, R. B.; Wehry, E. L. *J. Am. Chem. Soc.* **1972**, *94*, 946. (b) Posokhov, Y. O.; Kyrychenko, A.; Ladokhin, A. S. *Anal. Biochem.* **2010**, *407*, 284.

(14) Barone, V.; Cossi, M. *J. Phys. Chem. A* **1998**, *102*, 1995.

(15) Frisch, M. J.; Trucks, G. W.; Schlegel, H. B.; Scuseria, G. E.; Robb, M. A.; Cheeseman, J. R.; Scalmani, G.; Barone, V.; Mennucci, B.; Petersson, G. A.; Nakatsuji, H.; Caricato, M.; Li, X.; Hratchian, H. P.; Izmaylov, A. F.; Bloino, J.; Zheng, G.; Sonnenberg, J. L.; Hada, M.; Ehara, M.; Toyota, K.; Fukuda, R.; Hasegawa, J.; Ishida, M.; Nakajima,

T.; Honda, Y.; Kitao, O.; Nakai, H.; Vreven, T.; Montgomery, J. A., Jr.; Peralta, J. E.; Ogliaro, F.; Bearpark, M.; Heyd, J. J.; Brothers, E.; Kudin, K. N.; Staroverov, V. N.; Kobayashi, R.; Normand, J.; Raghavachari, K.; Rendell, A.; Burant, J. C.; Iyengar, S. S.; Tomasi, J.; Cossi, M.; Rega, N.; Millam, J. M.; Klene, M.; Knox, J. E.; Cross, J. B.; Bakken, V.; Adamo, C.; Jaramillo, J.; Gomperts, R.; Stratmann, R. E.; Yazyev, O.; Austin, A. J.; Cammi, R.; Pomelli, C.; Ochterski, J. W.; Martin, R. L.; Morokuma, K.; Zakrzewski, V. G.; Voth, G. A.; Salvador, P.; Dannenberg, J. J.; Dapprich, S.; Daniels, A. D.; Farkas, Ö.; Foresman, J. B.; Ortiz, J. V.; Cioslowski, J.; Fox, D. J. *Gaussian09*, revision A.1; Gaussian Inc.: Wallingford, CT, 2009.

(16) Safronov, A. V.; Shlyakhtina, N. I.; Hawthorne, M. F. *Organometallics* **2012**, *31*, 2764.

(17) Brown, H. C.; Ravindran, N. *J. Am. Chem. Soc.* **1973**, *95*, 2396.

(18) Van Dyke, D. A.; Pryor, B. A.; Smith, P. G.; Topp, M. R. *J. Chem. Educ.* **1998**, *75*, 615.

(19) Yang, J.; Lin, C.; Hwang, C. *Org. Lett.* **2001**, *31*, 889.

(20) Birks, J. B.; Dyson, D. J.; Munro, I. H. *Proc. R. Soc. London A* **1963**, *275*, 575.